Phys. Status Solidi RRL **10**, No. 7, 520–524 (2016) / **DOI** 10.1002/pssr.201600096

Fast and slow lifetime degradation in boron-doped Czochralski silicon described by a single defect

Brett Hallam[*,1], **Malcolm Abbott**[1], **Tine Nærland**[**,2], **and Stuart Wenham**[1]

[1] School of Photovoltaic and Renewable Energy Engineering, University of New South Wales, 2052 Sydney, Australia
[2] Institute for Energy Technology, Instituttveien 18, 2007 Kjeller, Norway

Received 10 April 2016, revised 22 May 2016, accepted 7 June 2016
Published online 10 June 2016

Keywords boron, oxygen, light-induced degradation, defects, Czochralski process, silicon

[*] Corresponding author: e-mail brett.hallam@unsw.edu.au, Phone: +61 2 93850411
[**] Now with Ira A. Fulton Schools of Engineering, Arizona State University, Tempe, AZ 85287, USA

A demonstration that boron–oxygen related degradation in boron-doped Czochralski silicon could be caused by a single defect with two trap energy levels is presented. In this work, the same two-level defect can describe the fast and slow lifetime decay with a capture cross-section ratio of electrons and holes for the donor level of $\sigma_n/\sigma_p = 19 \pm 4$. A model is proposed for the multi-stage degradation involving a single defect, in which the product of the slow reaction is a reactant in the fast reaction. After thermal processing, a population of interstitial oxygen (O_i) exists in a certain state (the precursor state) that can rapidly form defects (fast degradation) and another population of O_i exists in a state that is required to undergo a slow transformation into the precursor state before defect formation can proceed (slow degradation). Kinetic modelling is able to adequately reproduce the multi-stage degradation for experimental data. Dark annealing is also shown to impact the extent of 'fast' degradation. By decreasing the dark annealing time on pre-degraded wafers, a more severe 'fast' degradation of the samples can be enabled during subsequent illumination, consistent with this theory. The paper then discusses possible candidates for the chemical species involved.

1 Introduction The degradation of carrier lifetime in boron-doped Czochralski (Cz) silicon due to the formation of boron–oxygen (B–O) complexes has been shown to occur in two stages, with a 'fast' initial decay of lifetime, and a subsequent 'slow' decay [1]. A common understanding is that the fast and slow decay are caused by two different defects [2]. Evidence for this includes the determination of different capture cross-section ratios for electrons and holes (σ_n/σ_p) and the very different timescales of degradation [2]. However, some evidence exists for them being the same defect such as the fast and slow degradation rates having the same dependence on boron and interstitial oxygen (O_i) concentration [2] and the very similar values for acceptor and donor levels of the defects [3, 4]. Hypotheses related to the structure and formation of B–O defects have often assumed the existence of two separate defects. This has led to some contradictory explanations related to the fundamental nature of the defect, in particular the involvement of substitutional boron (B_s) and interstitial boron (B_i) [2, 4–9]. Other work studying the slow degradation in isolation has also led to many contradictions related to the structure and formation of B–O defects [10–13]. Furthermore, many of the published theories do not account for the recently identified donor and acceptor behaviour of the B–O defect during both the fast and slow decay [3, 4]. It is clear that further work is required to understand this defect and new insights into the nature of the fast and slow degradation may play an important role in unlocking it's true nature.

This paper proposes that the fast and slow degradation are in fact caused by the same defect whose recombination properties can be described by two trap levels within the band-gap (an acceptor and donor level). It is assumed that the defect is comprised of B_s and a certain species of O_i. The different rates of degradation observed occur due to a multi-stage defect formation process where the initial state of the silicon contains different percentages at each stage. More specifically, a certain population of defect precursors

(O_P) exists in the silicon that can enable a rapid formation of the defects, and that a latent interstitial oxygen species (O_L) exists in the silicon required to undergo a slow transformation into that precursor state before defect formation can proceed. Hence, the formation rate of O_P from O_L is much slower than the formation rate of the recombination active defect. We now investigate how well this hypothesis is able to explain the experimentally observed behaviour of the B–O defect. The concept that the ability to form defects is limited by the availability of defect precursors is similar to that demonstrated for the passivation of B–O defects whereby the passivation of the defects is limited by the availability of defects for passivation [14].

2 Experimental details To investigate the potential validity of this hypothesis, we use kinetic modelling to describe the full degradation process for lifetime test samples. Symmetrical lifetime samples were prepared on 325 µm thick boron-doped Cz silicon wafers with a doping density of $N_a = 3.6 \times 10^{15}/cm^3$. Wafers were RCA cleaned and a 40 nm layer of amorphous silicon was deposited on both sides using plasma enhanced chemical vapor deposition (PECVD). The wafers were dark annealed at 200 °C for 15 minutes to dissociate all B–O defects. The evolution of effective minority carrier lifetime (τ_{eff}) throughout light soaking at 303 ± 2 K was measured using an automated quasi-steady-state photoconductance (QSS-PC) tool with an externally controlled bias halogen lamp (approximately 50 mW/cm^2), to provide constant illumination in between measurements (see [15] for further details). Lifetimes presented were obtained at an excess carrier concentration of $\Delta n = 0.1 \cdot N_a$.

A 3-state model is used with normalized populations of O_L (N_L), O_P (N_P) and the formed B–O defects (N_{BO}). It is assumed that after dark annealing a certain initial population of N_L and N_P exist in the silicon such that $N_{L(t=0)} + N_{P(t=0)} = 1$, and $N_{BO(t=0)} = 0$. In the fully degraded state $N_L = N_P = 0$, and $N_{BO} = 1$. O_L can slowly transform into the defect precursor state O_P with a reaction rate k_{slow}, and O_P can form B–O defects with reaction rate k_{fast}. Hence, the total population of oxygen that can eventually lead to B–O defect formation is $O_X = O_L + O_P$. The differential equations for the model for defect formation are shown in Eqs. (1)–(3) below:

$$\frac{\partial N_L}{\partial t} = -k_{slow} \cdot N_L \,, \tag{1}$$

$$\frac{\partial N_P}{\partial t} = k_{slow} \cdot N_L - k_{fast} \cdot N_P \,, \tag{2}$$

$$\frac{\partial N_{BO}}{\partial t} = k_{fast} \cdot N_P \,. \tag{3}$$

The calculated lifetime is based on a dark annealed lifetime of $\tau_{eff,DA} = 1120$ µs and a fully degraded lifetime of $\tau_{eff,DG} = 120$ µs using Eq. (4):

$$\frac{1}{\tau_{eff}} = \frac{1}{\tau_{eff,DA}} - \frac{N_{Bo}}{\tau_{eff,DG}} \,. \tag{4}$$

To investigate the effect of dark annealing, symmetrical lifetime samples with PECVD silicon nitride were prepared on boron-doped Cz wafers ($N_a = 9 \times 10^{15}/cm^3$) with a gettering diffusion, alkaline texturing, screen print diffusion and subsequent thermal process to reduce the concentration of interstitial iron (Fe_i) to undetectable concentrations. Samples were fully degraded by light soaking under halogen lights with an illumination intensity of approximately 70 mW/cm^2 for 48 h at 30 °C. Subsequently, samples were dark annealed at approximately 160 °C for various durations to dissociate the B–O defects. Degradation was performed in-situ on a QSS-PC/QSS-PL tool.

3 Results and discussion Figure 1 shows the degradation in τ_{eff} during light soaking for a lifetime sample clearly highlighting the fast and slow decay. Red curves show the simulated minority carrier lifetime at $0.1 \cdot N_a$ for various fractions of O_X in the precursor state, O_P (indicated by the numbers in the graph for $N_{P(t=0)}$). As shown, if all O_X is in the O_L state ($N_{P(t=0)} = 0$), a slow degradation results with all O_X needing to go through the slow transition before defect formation can proceed. In contrast, if all O_X is in the O_P state ($N_{P(t=0)} = 1$), all precursors are available for defect formation and a rapid formation of defects results. For initial conditions with both O_L and O_P present, a two-stage degradation process results. For a value of $N_{P(t=0)} = 0.2$ (and $N_{L(t=0)} = 0.8$) the modeled lifetime curve closely matches the degradation data. That is 20% of O_X are available as precursors (O_P) and the remaining 80% are O_L requiring to first undergo a slow transition into the O_P state.

If the lifetime degradation observed above is due to a single defect then it should be possible to fit the injection level dependent effective lifetime data at every stage using the same two-level Shockley–Read–Hall defect. A selection of Auger-corrected inverse τ_{eff} ($1/\tau_{eff} - 1/\tau_{Aug}$) versus Δn curves from various stages of this degradation are

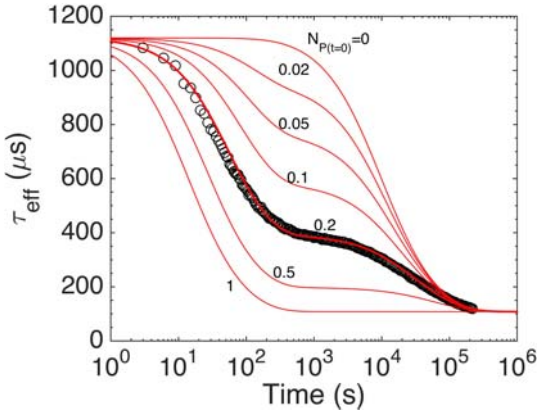

Figure 1 Lifetime data (black circles) for a degradation process at 303 K under 50 mW/cm^2. Red curves show simulations based on a dark annealed lifetime of 1120 µs and fully degraded lifetime of 120 µs for varying fractions of initially available defect precursors ($N_{P(t=0)}$) as indicated in the graph.

shown in Fig. 2(a). Curve fitting was used to separate different bulk and surface lifetime components at each stage of degradation [16]. This included a saturation current density (J_0) of 9 ± 1 fA/cm^2 and a fixed injection-level independent bulk lifetime ($\tau_{bulk,0}$) of 5 ms. Two separate Schockley–Read–Hall (SRH) defect trap levels were considered to represent the donor ($E_{trap,d}$) and acceptor levels ($E_{trap,a}$) of the B–O defect with 'negative U' properties [4]. Fixed trap levels and capture cross section ratios were assumed. The SRH trap levels used were $E_{trap,d}$ at 0.41 eV below the conduction band (E_c) [2] and $E_{trap,a}$ at 0.26 eV above the valence band (E_v) [3]. In each case the σ_n/σ_p value was fixed at 19.3 for $E_{trap,d}$, and 2.11 × 10^{-3} for $E_{trap,a}$ (consistent with Ref. [3]). The modeled SRH inverse lifetime components for electrons of $E_{trap,a}$ ($1/\tau_{SRHn,a}$) and $E_{trap,d}$ ($1/\tau_{SRHn,d}$) are shown in Fig. 2(b) as a function of the normalised defect density (NDD) using the measured τ_{eff} data and calculated using Eq. (5), assuming $\tau_{eff,DA}$ = 1120 µs:

$$\mathrm{NDD} = \frac{1}{\tau_{eff}} - \frac{1}{\tau_{eff,DA}}. \quad (5)$$

The curves show an excellent fit at the various stages of both the fast and slow lifetime decay, with the SRH inverse lifetime components scaling approximately linearly with the normalised defect density for both the acceptor and donor levels. Slight deviations from a pure linear correlation between the normalised NDD and the $\tau_{SRHn,a}$ and $\tau_{SRHn,d}$ values may be caused by a changing occupation of the different B–O defect charge states throughout the degradation process. Errors in the background $\tau_{bulk,0}$, $\tau_{eff,DA}$, $\tau_{eff,DG}$ and σ_n/σ_p values, or a modulation of other lifetime components throughout the process may have also contributed to differences. The determination of a single set of donor and acceptor SRH values all throughout the degradation cycle provides support for a single defect being responsible for the fast and slow B–O related degradation in boron-doped Cz material.

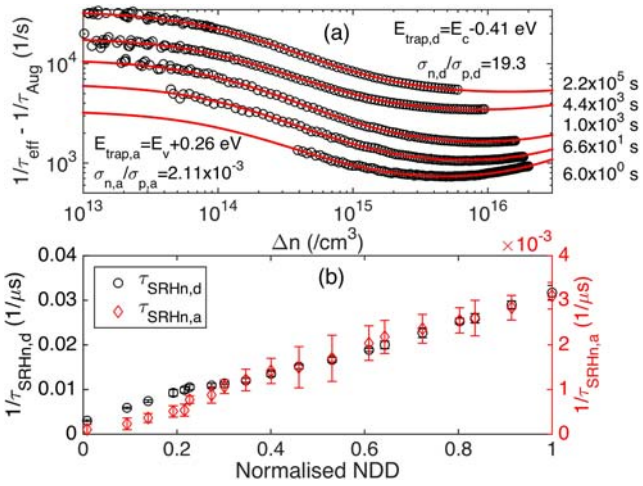

Figure 2 (a) Curves of Auger corrected inverse effective minority carrier lifetime ($1/\tau_{eff} - 1/\tau_{Aug}$) versus excess minority carrier density (Δn) after dark annealing and 50 mW/cm^2 illumination of various durations (indicated in the graph). Red curves show the modeled curves assuming values shown in the graph. (b) Correlation between the SRH electron lifetime components for the acceptor ($\tau_{SRHn,a}$) and donor level ($\tau_{SRHn,d}$) versus normalised NDD.

Whilst the hypothesis that B–O degradation is caused by a single defect is consistent with the results in this work, the results are inconsistent with some other reports in the literature. For example, the capture cross-section ratio used in modelling of σ_n/σ_p = 19.3 for $E_{trap,d}$ in this work is larger than that determined in previous work (σ_n/σ_p = 10) [2]. However, the value determined in previous work was obtained assuming a single trap energy level for the defect, and therefore did not include the influence of the subsequently identified acceptor level of the defect [4] in reducing τ_{eff} for higher Δn values due to the capture of holes. Hence the actual σ_n/σ_p of $E_{trap,d}$ is likely larger than 10. Furthermore, various studies have shown a range of values for σ_n/σ_p [17, 18]. Attempts to fit the curves in this work with σ_n/σ_p = 10, failed. A range of possible values for the σ_n/σ_p of $E_{trap,d}$ was determined as $16 < \sigma_n/\sigma_p < 23$ in order to obtain a reasonable visual fit to the data. The σ_n/σ_p for $E_{trap,d}$ determined in this work was also substantially lower than the previously determined value (σ_n/σ_p = 100) for the fast decay [2]. However several advancements have occurred in the last 10 years in relation to lifetime spectroscopy, such as understanding the influence of Fe_i in silicon with a known value of $\sigma_n/\sigma_p > 100$, which can be modulated during early stages of B–O defect formation processes, and is a common impurity in photovoltaic grade silicon [19]. Developments of wafer crystallization approaches and surface passivation have also led to the ability to achieve substantially higher lifetimes in this work, which therefore show less potential influence from other unrelated impurities.

To further investigate the kinetics of such as system, incremental dark annealing was performed. If the defect formation process requires the formation of the precursor, then dark annealing pre-degraded wafers would presumably transition the system from a state with all defects formed, back through the precursor state towards an equilibrium of O_P and O_L. The NDD after 100 s of light soaking is shown in Fig. 3, with a decreasing NDD for increasing durations of dark annealing. For short annealing times, the NDD was substantially higher than the typical value achieved after dark annealing for 10 min at 200 °C. This suggests that during dark annealing, first the defects dissociate, followed by a transition out of the precursor state O_P into another state, O_L. This provides further evidence the defect formation proceeds first through a slow reaction to form the defect precursor, followed by a more rapid reaction to form the B–O defect.

While the precursor theory presented above explains the observed lifetime trends, it is not clear what actual species of O_i is involved and this requires further studies. The majority of O_i in silicon is reported as monomers (O_{1i}) [20], and with only 20% of defects present after fast degradation, O_{1i} is unlikely to be O_P. Given the quadratic dependence of

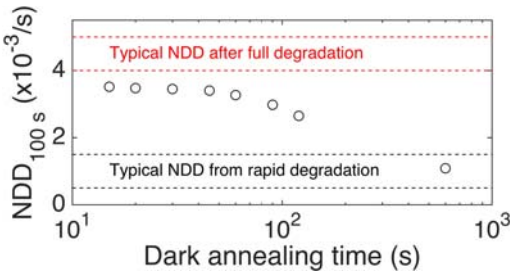

Figure 3 Normalised defect density (NDD) after 100 s of degradation on samples with prior full degradation and varying dark annealing times at 160 °C. Typical values of the NDD after rapid and full degradation on samples with a 10 min dark anneal at 200 °C are indicated in the graph.

the saturated defect concentration on (O_i) and the typically quadratic dependences of (O_{2i}) on total (O_i) [21], it would appear likely that O_{2i} is involved as a precursor (O_P) or a latent species (O_L) that can form O_P. Oxygen precipitate theory suggests that an equilibrium exists between O_{1i}, O_{2i} and the other small interstitial oxygen chains [22]. It is likely that carrier injection could alter this equilibrium and enhance the diffusivity of various oxygen species through the lattice, and explain the electron dependence in the defect formation rate. The involvement of charge-state driven O_{2i} migration in defect formation has been presented previously [10]. Whilst recent attempts to measure specific O_{2i} charge state species were unsuccessful, therefore questioning this theory [21], the potential involvement of metastable charge states and the modulation of charge state concentrations with minority carrier injection were not considered. These attributes and subsequent influence on diffusivity are well known for other impurities such as atomic hydrogen [23, 24].

Hence, it is possible that the growth or dissolution of a range of small interstitial oxygen chains such as O_{2i}, trimers (O_{3i}) and tetramers (O_{4i}) can enable defect formation. This could also explain observations by Voronkov et al. where it was concluded O_{2i} was not involved as a defect precursor, whereby annealing with conditions known to reduce (O_{2i}) through the generation of O_{3i} did not reduce the saturated defect concentration [12]. The annealing may have simply shifted the fractions of O_X in the O_L and O_P states, without leading to a change in the total O_X concentration.

Whilst highly speculative, a possible candidate for the defect precursor is the O_{3i}, and that the involvement of O_{2i} is through the capture of relatively immobile O_{1i}. Calculated migration and binding energies for O_{2i} and O_{3i} are in the vicinity of the activation energies determined for the fast and slow B–O related degradation [2, 25]. This would suggest that a possible defect structure is a complex of B–O_{3i}. The involvement of O_{3i} and a defect structure of B–O_{3i} was previously proposed [26], however in that study it was suggested that degradation was caused by a reconfiguration of a latent B–O defect under illumination, i.e. the defect precursor was proposed as a latent B–O_{3i} complex.

The independence of the reaction rates on (O_i) may indicate that the actual capture of O_{1i} by O_{2i} is not the rate-limiting reaction, but rather the rate-limiting reaction is related to the migration of O_{2i} and/or O_{3i}. Furthermore, the square dependence of the fast reaction on total hole concentration [27] may suggest that the fast reaction is not actually the formation of a B–O defect, but rather, that the defect formation occurs in a subsequent, and even more rapid reaction. This is consistent with the hypothesis of a single defect being responsible for lifetime degradation in boron-doped Cz silicon, with the slow reaction being a precursor of one or more fast reactions. The dependence of degradation rates on electron/hole concentrations will be discussed in a future publication.

4 Conclusion A demonstration that the B–O related degradation in boron-doped Cz silicon could be caused by a single defect with two trap energy levels was presented. Here, the same two-level SRH defect could describe the fast and slow lifetime decay with $\sigma_n/\sigma_p = 19 \pm 4$ for the donor level. This value greatly differs from the currently understood value of approximately 10 for the slow decay and 100 for the fast decay. A model was proposed to explain the multi-stage degradation cycle involving a single defect in which the product of the slow reaction is a reactant in the fast reaction. After thermal processing such as dark annealing, a certain population of O_i exists in the silicon that can rapidly form defects (fast degradation) and another population of O_i exists in a state that is required to undergo a slow transformation into the precursor state before defect formation can proceed (slow degradation). Dark annealing was shown to influence the extent of 'fast' degradation, with reduced dark annealing durations on pre-degraded samples leading to a more severe 'fast' degradation, consistent with this theory.

Acknowledgements This Program has been supported by the Australian Government through the Australian Renewable Energy Agency (ARENA) and the Australian Center for Advanced Photovoltaics (ACAP). The views expressed herein are not necessarily the views of the Australian Government, and the Australian Government does not accept responsibility for any information or advice contained herein. T. U. Nærland acknowledges funding from "The Norwegian Research Centre for Solar Cell Technology" and REC Wafer, REC Solar, Elkem Solar and the Norwegian Research Council through the KMB project "Defect engineering for crystalline silicon solar cells". The authors would like to thank the commercial partners of the ARENA 1-A060 project, and the UK Institution of Engineering and Technology (IET) for their funding support for this work through the A. F. Harvey Engineering Prize. The authors would also like to acknowledge the assistance of Moonyong Kim and Nicholas Gorman for their assistance with wafer processing.

References

[1] S. Rein, T. Rehrl, W.Warta, S. Glunz, and G. Willeke, Proceedings of the 17th European PVSEC, p. 1555 (2002).
[2] K. Bothe and J. Schmidt, J. Appl. Phys. **99**(1), 013701 (2006).

[3] T. Niewelt, J. Schön, J. Broisch, W. Warta, and M. Schubert, Phys. Status Solidi RRL **9**(12), 692–696 (2015).
[4] V. Voronkov, R. Falster, K. Bothe, B. Lim, and J. Schmidt, J. Appl. Phys. **110**(6), 063515 (2011).
[5] V. Voronkov, R. Falster, B. Lim, and J. Schmidt, ECS Trans. **50**(5), 123–136 (2013).
[6] M. Forster, E. Fourmond, F. Rougieux, A. Cuevas, R. Gotoh, K. Fujiwara, S. Uda, and M. Lemiti, Appl. Phys. Lett. **100**(4), 042110 (2012).
[7] C. Möller and K. Lauer, Phys. Status Solidi RRL **7**(7), 461–464 (2013).
[8] V. Voronkov and R. Falster, Solid State Phenom. **205**, 3–14 (2013).
[9] V. Voronkov and R. Falster, Phys. Status Solidi B (2016), DOI 10.1002/pssb.201600082.
[10] J. Schmidt and K. Bothe, Phys. Rev. B **69**(2), 024107 (2004).
[11] V. Voronkov, R. Falster, B. Lim, and J. Schmidt, J. Appl. Phys. **112**(11), 113717 (2012).
[12] V. V. Voronkov, R. Falster, K. Bothe, and B. Lim, Energy Proc. **38**, 636–641 (2013).
[13] T. Mchedlidze and J. Weber, Phys. Status Solidi RRL **9**(2), 108–110 (2015).
[14] B. Hallam, M. Abbott, N. Nampalli, P. Hamer, and S. Wenham, J. Appl. Phys. **119**, 065701 (2016).
[15] T. Nærland, H. Haug, H. Angelskar, R. Sondena, E. Marstein, and L. Arnberg, IEEE J. Photovolt. **3**(4), 1265–1270 (2013).
[16] A. Cuevas and D. Macdonald, Sol. Energy **76**(1), 255–262 (2004).
[17] X. Wang, M. Juhl, M. Abbott, Z. Hameiri, Y. Yao, and A. Lennon, Energy Proc. **55**, 169–178 (2014).
[18] J. Schmidt and A. Cuevas, J. Appl. Phys. **86**(6), 3175–3180 (1999).
[19] D. Macdonald, L. Geerligs, and A. Azzizi, J. Appl. Phys. **95**(3), 1021–1028 (2004).
[20] J. Murphy, The properties of nitrogen and oxygen in silicon, Ph.D. thesis, University of Oxford (2006).
[21] L. I. Murin, E. A. Tolkacheva, V. P. Markevich, A. R. Peaker, B. Hamilton, E. Monakhov, B. G. Svensson, J. L. Lindstrom, P. Santos, J. Coutinho, and A. Carvalho, Appl. Phys. Lett. **98**(18), 182101 (2011).
[22] N. Inoue, J. Osaka, and K. Wada, J. Electrochem. Soc. **129**(12), 2780–2788 (1982).
[23] C. Herring, N. Johnson, and C. Van de Walle, Phys. Rev. B **64**(12), 125209 (2001).
[24] D. Mathiot, Phys. Rev. B **40**(8) 5867–5870 (1989).
[25] Y. J. Lee, J. Von Boehm, M. Pesola, and R. M. Nieminen, Phys. Rev. B **65**(8), 085205 (2002).
[26] J. Bourgoin, N. Angelis, and G. Strobl, Proceedings of the 16th European Photovoltaic Solar Energy Conference, p. 1356 (2000).
[27] J. Schön, T. Niewelt, J. Broisch, W. Warta, and M. Schubert, J. Appl. Phys. **118**, 245702 (2015).

